Channel Access Algorithms with Active Link Protection for Wireless Communication Networks with Power Control

Nicholas Bambos, *Member, IEEE*, Shou C. Chen, *Member, IEEE*, and Gregory J. Pottie, *Member, IEEE*

***Abstract*—A distributed power-control algorithm with active link protection (DPC/ALP) is studied in this paper. It maintains the quality of service of operational (active) links above given thresholds at all times (link quality protection). As network congestion builds up, established links sustain their quality, while incoming ones may be blocked and rejected. A suite of admission control algorithms, based on the DPC/ALP one, is also studied. They are distributed/autonomous and operate using local interference measurements.**

A primarily networking approach to power control is taken here, based on the concept of active link protection, which naturally supports the implementation of admission control. Extensive simulation experiments are used to explore the network dynamics and investigate basic operational effects/tradeoffs related to system performance.

***Index Terms*—Admission control, multiple access, power control, radio channel access, wireless networks.**

I. Introduction

ADAPTIVE control of transmitter powers allows communication links to be established in a channel, using minimum power to achieve required signal-to-interference ratios (SIR) reflecting given quality of service (QoS) levels. Interference mitigation increases network capacity through higher channel reuse.

Early works on power control [1], [2] focused on balancing (equalizing) the SIRs on all radio links, maximizing the minimum SIR through centralized operations. Later, distributed SIR-balancing algorithms [3], [4] were developed. The SIR-balancing approach makes difficult to differentiate link QoS requirements and guarantee them. In a dynamic network environment, it may require removal of some active links to increase the QoS on others [15]. Other algorithms can exercise admission control [5], [6], [14] and provide differentiated QoS guarantees, but require some degree of centralized decision-making.

Foschini and Miljanic [7], [8] and Mitra [11] proposed a distributed asynchronous on-line power control algorithm, which can incorporate user-specific SIR requirements and yield minimal transmitter powers to satisfy them. It converges geometrically fast, when the users have compatible SIR requirements. However, as new users try to access the channel, the SIRs of existing ones may fluctuate below the required thresholds and cause inadvertent dropping of ongoing calls [23], [25]. If the SIR requirements are infeasible, the algorithm will diverge (in the unconstrained power case). More recently developed algorithms on constrained power control [16], [27], [28] utilize various techniques for dealing with the infeasibility problem.

In this paper, we take a networking approach to the design of power control algorithms, where the issue of admission control is made central. We introduce an active link protection (ALP) mechanism, which sustains the SIR of active links above required thresholds, as new links are accessing the channel. Intuitively speaking, new links power up gradually (in a guarded manner) while active ones are endowed with an SIR protection margin, which cushions the effect of increased interference due to new links entering the channel. This becomes clear in the following sections. Initial efforts in exploring this approach were partially presented in our earlier works [9], [10], [30] and a high-level review in [21].

In [17] an alternative interesting approach was later investigated for admission-centric power control. Considering the uplink (the downlink is analogous) of a cellular architecture, the idea in [17] is that a single incoming mobile, seeking admission into a specific channel, monitors pilot tones from all the interacting base stations in that channel in order to measure the base-to-mobile (downlink) power gains. It then assumes that those are equal to the mobile-to-base uplink power gains (reciprocity assumption). Moreover, for *each existing* mobile-to-base uplink in the channel, the following information is communicated to *all other* uplinks in the channel, including the new one considered for admission: 1) the receiver's thermal noise level; and 2) the transmitter's power level. Based on that global information, all uplinks compute the maximum amount (ϵ_k in [17]) they can proportionally scale up their powers without violating any power constraint. Starting from these scaled-up powers, they follow a power-relaxation algorithm, analogous to the one in [7], until they reach equilibrium. If the new link has been admitted, by achieving its required SIR, the algorithm stops. If not, another phase of the previous process starts from the current power equilibrium with a new collective computation of the scale-up parameter. This is repeated until the new uplink is admitted or the maximum power constraint

Manuscript received October 9, 1998; revised May 8, 1999; approved by IEEE/ACM TRANSACTIONS ON NETWORKING Editor J. Daigle. This work was supported in part by the National Science Foundation.

N. Bambos is with the Department of Electrical Engineering and the Department of Management Science and Engineering, Stanford University, Stanford, CA 94305 USA (e-mail: bambos@stanford.edu).

S. C. Chen is with Trillium Digital Systems, Los Angeles, CA 90025 USA.

G. J. Pottie is with the Department of Electrical Engineering, University of California, Los Angeles, CA 90024 USA (e-mail: pottie@ee.ucla.edu).

Publisher Item Identifier S 1063-6692(00)09119-6.

of an uplink is hit, in which case the new uplink is rejected. As mentioned, above it is assumed that only one new uplink is trying for admission at a time.

The suite of algorithms presented in this paper does not require any interlink communication, collective/centralized computation, the reciprocity assumption, or the single admission trial one. They are designed to be fully distributed and autonomous (at the individual link level), and work with multiple new links seeking admission concurrently. The total lack of global communication/computation is traded for a slight reduction in network capacity (getting, however, a slightly higher link SIR performance), and a rare possibility of error events, which are controllable and easy to recover from. With the introduction of minimal interlink communication, the latter are eliminated. The main two key ideas of this approach are: 1) the *gradual power-up* of new links entering the channel; and 2) the introduction of a performance *protection margin* cushioning the links already in it. Those are implemented into a system level methodology for active link protection and distributed admission control, which is supported by an autonomous drop-out/retrial mechanism (voluntary and/or forced), diffusing local hot-spots and smoothing out the network dynamics.

The organization of this paper is as follows. In Section II the modeling framework is defined and in Section III the power control algorithm of Foschini and Miljanic [7] is briefly reviewed. In Section IV we introduce the distributed power control with active link protection (DPC/ALP) algorithm and establish its key properties. Link admission control based on DPC/ALP is discussed in Sections V and VI. The case of constrained transmitter powers is treated in Section VII and the issue of start-up power in Section VIII. The presented suite of algorithms (DPC/ALP/VDO/FDO) provides an integrated framework for admission control, based on power control. Complex dynamical effects associated with network-wide operation of the algorithms are discussed in a simulation study presented in Section IX. Extensions and issues for further research are mentioned in Section X.

The focus of this study is on the power adaptation dynamics of the wireless network. Following standard practice in this line of research, it is implicitly assumed that the time scale of mobility is much larger than that of power adaptation and the network structure is quasi-static, not changing significantly between power updates. On the other hand, the transmission time scale is much shorter than that of power adaptation, so that a large enough number of bits is transmitted between two power updates to allow reliable estimation of (average) interference values and "wash out" short-term statistical fluctuations at that level.

II. The Wireless Network as a Collection of Interfering Radio Links

We consider the wireless network to be a collection of radio links. This is the appropriate level of modeling abstraction in this study. Each link corresponds to a single-hop radio transmission from a transmitter node to an intended receiver node. Chains of consecutive links may correspond to multihop communication paths, but we can still consider them as collections of individual links for our purposes. There may be many communication channels, but we assume that the interference between links operating in different ones is negligible. That is, channels are orthogonal and network dynamics in different ones decouple, so only co-channel interference need be considered. We can therefore reduce the network picture to that of a collection of *interfering links* in a *single channel*, rendering the notions of *network admission* and *channel access* equivalent.

In the cellular communication network paradigm, links correspond to up-stream and down-stream transmissions between mobiles and base stations. In the *ad-hoc* networking paradigm, links may correspond to single-hop transmissions between laptop computers (or other mobile and/or static infrastructure). In FDMA systems, the channels are nonoverlapping frequency bands. In spread-spectrum systems [20], the whole spectrum can be viewed as a single channel and interference basically reflects cross-correlation effects between codes in CDMA transmission.

Generally speaking, the transmission quality (bit error rate) of a network link is a decreasing function of the SIR at its receiver node. Given that there are $N \in \mathcal{Z}_+$ interfering links in the channel (network), we denote the SIR of the ith link by

$$R_i = \frac{G_{ii}P_i}{\sum_{j\neq i} G_{ij}P_j + \eta_i}, \quad i, j \in \{1, 2, 3, \ldots, N\}. \tag{1}$$

$G_{ij} > 0$ is the power gain (actually loss) from the transmitter of the jth link to the receiver of the ith one. It includes the free space loss, multipath fading, shadowing, and other radio-wave propagation effects, as well as the processing gain in the case of spread-spectrum transmission. It is specified by the particular propagation model of the channel. Let P_i be the power transmitted from the ith link's transmitter node and $\eta_i > 0$ the thermal noise power at its receiver node.

For each link i there is some SIR threshold requirement $\gamma_i > 0$, reflecting some minimal QoS that the link must support throughout the transmission in order to operate properly. Therefore, we need to have

$$R_i \geq \gamma_i, \quad i \in \{1, 2, 3, \ldots, N\}. \tag{2}$$

In matrix form, the SIR requirements (1), (2) can be written as

$$(\mathbf{I} - \mathbf{F})\mathbf{P} \geq \mathbf{u} \quad \text{and} \quad \mathbf{P} > 0, \tag{3}$$

where $\mathbf{P} = (P_1, P_2, \ldots P_i, \ldots P_N)'$ is the column vector of transmitter powers, and

$$\mathbf{u} = \left(\frac{\gamma_1\eta_1}{G_{11}}, \frac{\gamma_2\eta_2}{G_{22}}, \frac{\gamma_3\eta_3}{G_{33}}, \ldots, \frac{\gamma_i\eta_i}{G_{ii}}, \ldots, \frac{\gamma_N\eta_N}{G_{NN}}\right)' \tag{4}$$

is the column vector of noise powers, rescaled by SIR requirements and link power gains, and finally, $\mathbf{F}$ is the matrix with entries

$$F_{ij} = \begin{cases} 0, & \text{if } i = j \\ \dfrac{\gamma_i G_{ij}}{G_{ii}}, & \text{if } i \neq j \end{cases} \tag{5}$$

where $i, j \in \{1, 2, 3, \ldots, N\}$. The latter is the matrix of cross-link power gains (appropriately rescaled).

We briefly point out below a few standard facts we use later. The matrix $\mathbf{F}$ has nonnegative elements and it is reasonable to assume that is *irreducible*, since we are not considering totally isolated groups of links that do not interact with each other. Therefore, by the Perron–Frobenius theorem [19], [22], [11], we have that the maximum modulus eigenvalue of $\mathbf{F}$ is real, positive, and simple, while the corresponding eigenvector is positive componentwise. Denote the *maximum modulus eigenvalue* of $\mathbf{F}$ by ρ_F. We then have the following well-known fact from standard matrix theory.

Fact 2.1 (Existence of a Feasible Power Vector): The following statements are equivalent:

1) There exists a power vector $\mathbf{P} > 0$ such that $(\mathbf{I} - \mathbf{F})\mathbf{P} \geq \mathbf{u}$.
2) $\rho_F < 1$.
3) $(\mathbf{I} - \mathbf{F})^{-1} = \sum_{k=0}^{\infty} \mathbf{F}^k$ exists and is positive componentwise.

Since ρ_F is the maximum modulus eigenvalue of $\mathbf{F}$, if $\rho_F < 1$, then

$$\lim_{k \to \infty} \mathbf{F}^k = 0. \tag{6}$$

Also, if (3) has a solution, then

$$\mathbf{P}^* = (\mathbf{I} - \mathbf{F})^{-1}\mathbf{u} \tag{7}$$

is a Pareto-optimal solution of (3), in the sense that any other $\mathbf{P}$ satisfying (3) would require as much power from every transmitter [11], i.e.

$$\mathbf{P} \geq \mathbf{P}^* \tag{8}$$

componentwise. Therefore, if it is possible to satisfy the SIR requirements for all links simultaneously, a good power control strategy is to set the transmitter powers to $\mathbf{P}^*$, so as to minimize the power spent.

III. Distributed Power Control (DPC) Based on Local SIR Measurements

Foschini and Miljanic have proposed the following DPC algorithm [7]:

$$\mathbf{P}(k+1) = \mathbf{F}\mathbf{P}(k) + \mathbf{u} \tag{9}$$

$k = 1, 2, 3, \ldots$, which converges to $\mathbf{P}^*$ (*when that exists*). Indeed, by recursively substituting into (9) we get $\mathbf{P}(k) = \mathbf{F}^k\mathbf{P}(0) + [\sum_{i=0}^{k-1} \mathbf{F}^i]\mathbf{u}$, which gives

$$\begin{aligned}\lim_{k \to \infty} \mathbf{P}(k) &= \lim_{k \to \infty} [\mathbf{F}^k]\mathbf{P}(0) + \lim_{k \to \infty} \left[\sum_{i=0}^{k-1} \mathbf{F}^i\right]\mathbf{u} \\ &= 0 + \left[\sum_{i=0}^{\infty} \mathbf{F}^i\right]\mathbf{u} \\ &= (\mathbf{I} - \mathbf{F})^{-1}\mathbf{u} = \mathbf{P}^* \end{aligned} \tag{10}$$

if $\rho_F < 1$ (using Fact 2.1). If not, the powers diverge to infinity. The first term in (9) relates to cross-link interference, while the second to intrinsic noise (both rescaled by G_{ii}). Interesting extensions of (9) have been proposed by Mitra [11]–[13] (asynchronous implementation, bursty transmissions, multiclass traffic), Yates *et al.* [25]–[27] (constrained powers, joint power control and base station assignment), Andersin *et al.* [15], [16], [18], and Hanly [23], [24].

The above DPC algorithm can be simplified, so that it is not necessary to make separate local measurements of co-channel interference $\sum_{i \neq j} G_{ij}P_j$, noise power η_i, and propagation gain G_{ii}. Actually, only the SIR at the receiver R_i is needed. Indeed, we first observe that according to (9) the power updates for the ith link can be written as $P_i(k+1) = (\gamma_i/G_{ii})(\sum_{j \neq i} G_{ij}P_j(k) + \eta_i)$. However, from (1), we have $\sum_{j \neq i} G_{ij}P_j(k) + \eta_i = (G_{ii}P_i(k)/R_i(k))$, so substituting in the previous expression, we get the following simplified form of the DPC algorithm (9):

$$P_i(k+1) = \frac{\gamma_i}{R_i(k)} P_i(k) \tag{11}$$

for every link $i \in \{1, 2, 3, \ldots, N\}$. Therefore, each link independently increases its power when its current SIR is below its target value γ_i, and decreases it otherwise, trying to exactly meet its required SIR threshold. Of course, since all other links do the same, the objective is achieved only at the limit $k \to \infty$ (if feasible).

A comment clarifying what *distributed* means here is in order. Note that the basic object of the network model is the link, hence, "distributed" implies per individual link. Each link's receiver measures the interference and communicates this information to its transmitter, which then decides how to adjust its power. This feedback information transfer occurs on a separate network control channel or a low-rate reverse link (which also carries acknowledgments, etc.) In cellular networks, it can be piggybacked on the up-link (down-link). The important point is that this control traffic is minimal (one number per power update). Each link decides autonomously how to adjust its power based on information collected on it exclusively. Therefore, the decision-making is fully distributed at the link level.

IV. Distributed Power Control with Active Link Protection (DPC/ALP)

As easily seen, the DPC algorithm (9) and its simplified version (11) allow fluctuations of the link SIRs below the thresholds γ_i during their evolution. As a result, when new links try to access the channel (seeking admission to the network) established ones may be inadvertently dropped, due to transient fluctuations of their SIR (QoS) below γ. This may happen even if the new links can eventually be accommodated in steady state. If they cannot, all links will eventually degrade below their required γ and be rendered inoperative. Instead, we need a power control scheme which provides protection for links that are currently operational, maintaining their SIRs above the required thresholds γ_i at all times, as new links try to enter the network. Moreover, if the latter cannot be accommodated they are simply suppressed, without hurting the operational links in the process.

We design an algorithm for distributed power control with active link protection (DPC/ALP), which updates transmitter powers in steps (time slots) indexed by $k = 1, 2, 3, \ldots$, as follows. Let $\mathcal{L}$ be the set of all links and call a link $i \in \mathcal{L}$ **active** or **operational** during the kth step iff

$$R_i(k) \geq \gamma_i, \tag{12}$$

where $R_i(k)$ is its measured SIR in that time slot. $\mathcal{A}_k$ is the set of all active links during the kth step. Alternatively, call a link $i \in \mathcal{L}$ **inactive** or **new** during the kth step iff

$$R_i(k) < \gamma_i. \tag{13}$$

$\mathcal{B}_k$ is the set of all inactive links during the kth step. We also need a control parameter δ, such that

$$\delta = 1 + \epsilon > 1 \tag{14}$$

($\epsilon > 0$), arbitrarily chosen at this point, which in practice is slightly higher than 1. The algorithm is specified as follows:

1) Algorithm 1—Distributed Power Control with Active Link Protection (DPC/ALP): The algorithm operates by updating transmitter powers $P_i(k+1)$ at the $(k+1)$th step according to the following rule:

$$P_i(k+1) = \begin{cases} \dfrac{\delta\gamma_i}{R_i(k)} P_i(k), & \text{if } i \in \mathcal{A}_k \\ \delta P_i(k) = \delta^{(k+1)} P_i(0), & \text{if } i \in \mathcal{B}_k \end{cases} \tag{15}$$

or equivalently

$$P_i(k+1) = \begin{cases} \dfrac{\delta\gamma_i}{G_{ii}} I_i(k), & \text{if } i \in \mathcal{A}_k \\ \delta P_i(k) = \delta^{(k+1)} P_i(0), & \text{if } i \in \mathcal{B}_k \end{cases} \tag{16}$$

where

$$I_i(k) = \sum_{j \in \mathcal{A}_k \bigcup \mathcal{B}_k - \{i\}} G_{ij} P_j(k) + \eta_i \tag{17}$$

is the interference (plus noise) at the ith link's receiver during the kth update and $P_i(0) > 0$ is the initial power of its transmitter.

Note that in DPC/ALP active links $\mathcal{A}_k$ update their powers according to the standard DPC rule (11)—but shooting for an enhanced target $\delta\gamma_i$—while new ones $\mathcal{B}_k$ power up gradually at geometric rate δ. DPC/ALP artificially raises the SIR target to $\delta\gamma$ to provide a **protection margin** $\epsilon = \delta - 1$ for active links. This allows them to absorb the degrading effect of new ones powering up in the channel without dropping below their true targets γ. It cushions them against the jolts induced by new links. The latter **power up gradually**, inducing a limited degradation on active ones per step and giving them enough time to react. The DPC/ALP algorithm has some important properties which are established below.

Proposition 4.1 (SIR Protection of Active Links): For any fixed $\delta \in (1, \infty)$, we have that for every $k \in \{0, 1, 2, 3, \ldots\}$ and every $i \in \mathcal{A}_k$

$$R_i(k) \geq \gamma_i \Rightarrow R_i(k+1) \geq \gamma_i, \tag{18}$$

under the DPC/ALP power updating algorithm. Therefore

$$i \in \mathcal{A}_k \Rightarrow i \in \mathcal{A}_{k+1} \tag{19}$$

or equivalently

$$\mathcal{A}_k \subseteq \mathcal{A}_{k+1} \tag{20}$$

and

$$\mathcal{B}_{k+1} \subseteq \mathcal{B}_k \tag{21}$$

for every $k \in \{0, 1, 2, 3 \ldots\}$.

Proof: Using (1) and (16), we see that for every $i \in \mathcal{A}_k$

$$R_i(k+1) = \frac{\delta\gamma_i I_i(k)}{I_i(k+1)} \tag{22}$$

where $I_i(k) = \sum_{j \in \mathcal{A}_k - \{i\}} G_{ij} P_j(k) + \sum_{j \in \mathcal{B}_k} G_{ij} P_j(k) + \eta_i$. Moreover, using (15), we get $I_i(k+1) = \sum_{j \in \mathcal{A}_k - \{i\}} G_{ij} (\delta\gamma_j / R_j(k)) P_j(k) + \sum_{j \in \mathcal{B}_k} G_{ij} \delta P_j(k) + \eta_i$. Now, since $\gamma_j / R_j(k) \leq 1$ for every $i \in \mathcal{A}_k$ and $\eta_i/\delta < \eta_i$ (since $\delta > 1$), we get

$$\begin{aligned} I_i(k+1) = \delta \Bigg[& \sum_{j \in \mathcal{A}_k - \{i\}} G_{ij} \left(\gamma_j / R_j(k)\right) P_j(k) \\ & + \sum_{j \in \mathcal{B}_k} G_{ij} P_j(k) + (\eta_i / \delta) \Bigg] \\ \leq \delta I_i(k) & \end{aligned} \tag{23}$$

which proves (18), by substituting into (22). The rest follows trivially, completing the proof. ■

Proposition 4.1 shows that initially active links remain active throughout the DPC/ALP evolution. However, as seen later, initially inactive ones may become active at some point in time (and remain so forever after or until they complete their intended communication). This property supports naturally the notion of admitting new links into the network if/when they become active, which is the key aspect of our approach.

Proposition 4.2 (Bounded Power Overshoot): For any fixed $\delta \in (1, \infty)$, we have

$$P_i(k+1) \leq \delta P_i(k) \tag{24}$$

for every $k \in \{0, 1, 2, 3 \ldots\}$ and every $i \in \mathcal{A}_k$ under the DPC/ALP power updating algorithm.

Proof: By definition, $i \in \mathcal{A}_k$ implies that $R_i(k) \geq \gamma_i$. Therefore, $(\gamma_i / R_i(k)) \leq 1$ and from (15) the result follows immediately. ■

This shows that the overshoots of the DPC/ALP algorithm are bounded by δ [i.e. $((P_i(k+1))/P_i(k)) \leq \delta = 1 + \epsilon$], which is typically slightly larger than 1. Therefore, the powers of active links can only increase smoothly to accommodate the new links that are powering up in the channel.

Proposition 4.3 (Non-Active Link SIR Increases): For any fixed $\delta \in (1, \infty)$, we have

$$R_i(k) \leq R_i(k+1) \tag{25}$$

for every $k \in \{0, 1, 2, 3 \ldots\}$ and every $i \in \mathcal{B}_k$ under the DPC/ALP power updating algorithm.

Proof: Using (1) and (15), we have for every $i \in \mathcal{B}_k$ that

$$R_i(k+1) = \frac{G_{ii} \delta P_i(k)}{I_i(k+1)}. \tag{26}$$

Arguing as in the proof of Proposition 4.1, we see that $I_i(k+1) \le \delta I_i(k)$, and substituting in (26), we get

$$R_i(k+1) \ge \frac{G_{ii}P_i(k)}{I_i(k)} = R_i(k). \tag{27}$$

This completes the proof of Proposition 4.3. ■

Therefore, the SIR of every currently inactive (new) link is nondecreasing during each step of the DPC/ALP algorithm and so it may eventually rise above its required threshold, in which case the link becomes active and remains so forever after. The inherent geometric convergence of plain DPC, together with the geometric power-up of new links under DPC/ALP guarantee that the latter algorithm also converges geometrically fast. If δ is very small (too close to 1), it will dominate the convergence speed of DPC/ALP. If δ is large enough, the inherent speed of plain DPC takes over.

V. Admission of New Links into the Wireless Network Under DPC/ALP

We next focus on the dynamics of the DPC/ALP algorithm with respect to activation of new links. As mentioned before, we consider a new link to have been *admitted* to the network (channel) when it becomes active, raising its SIR above the threshold requirement; it then stays active forever, that is, until it completes its intended communication.

We first prove a "counter-proposition" which illustrates the behavior of the algorithm when no inactive link ever becomes activated under DPC/ALP; in this case we call the set of new links **totally inadmissible**. This proposition is used later to show that, if there is a feasible power configuration under which all links (active and new) can satisfy their actual SIR requirements, then the DPC/ALP algorithm will eventually activate all originally inactive links.

We consider a group of $N+M$ links, such that originally the ones in the set

$$\mathcal{A}_0 = \{1, 2, 3, \ldots, N-1, N\} \tag{28}$$

are active, while the ones in the set

$$\mathcal{B}_0 = \{N+1, N+2, N+3, \ldots, N+M-1, N+M\} \tag{29}$$

are inactive (new). We are mainly interested in whether the new links will eventually become active.

Proposition 5.1 (Totally Inadmissible New Links): Given that the network operates under the DPC/ALP algorithm, if

$$\mathcal{A}_k = \mathcal{A}_0 \neq \emptyset \quad \text{and} \quad \mathcal{B}_k = \mathcal{B}_0 \neq \emptyset \tag{30}$$

for every $k \in \{1, 2, 3, \ldots\}$, then the following limits exist:

$$\lim_{k\to\infty} R_i(k) = R_i^* < \infty \tag{31}$$

and

$$\lim_{k\to\infty} \frac{P_i(k)}{\delta^k} = D_i^* < \infty \tag{32}$$

for some positive constant D_i^*, for each $i \in \mathcal{A}_0 \cup \mathcal{B}_0$. Moreover

$$R_i^* = \gamma_i \quad \text{for every initially active link } i \in \mathcal{A}_0, \tag{33}$$

while

$$R_i^* \le \gamma_i \quad \text{for every initially inactive link } i \in \mathcal{B}_0. \tag{34}$$

Thus, if no link is ever admitted ($\mathcal{B}_k = \mathcal{B}_0$ for every future step k), then: 1) the SIRs of the initially active links are squeezed down to their lowest acceptable values γ; 2) the SIRs of all new links saturate below their required thresholds γ; while 3) the transmission powers of all links explode geometrically to infinity.

Proof: We have $N + M$ links such that $\mathcal{A}_0 = \{1, 2, 3, \ldots, N-1, N\}$ are active (already operational) and $\mathcal{B}_0 = \{N+1, N+2, N+3, \ldots, N+M-1, N+M\}$ are inactive (new). Since links in $\mathcal{B}_0$ remain forever inactive, we have from (15) that

$$\frac{P_i(k)}{\delta^k} = P_i(0) = D_i^* < \infty \quad \text{for every } i \in \mathcal{B}_0 \tag{35}$$

and for every $k \in \mathcal{Z}_+$, while from Proposition 4.3 we get

$$R_i(k) \le R_i^* \le \gamma_i \quad \text{for every } i \in \mathcal{B}_0 \tag{36}$$

due to increasingness of the SIRs of inactive links and the fact that they remain so forever.

We now need to study the behavior of active links. We first define

$$\mathbf{P}_a(k) = (P_1(k), P_2(k), \ldots, P_i(k), \ldots, P_N(k))' \tag{37}$$

to be the vector of powers of active links and

$$\mathbf{P}_n(k) = (P_{N+1}(k), P_{N+2}(k), \ldots, P_{N+M}(k))' \tag{38}$$

the vector of powers of inactive (new) ones. Observe that

$$\mathbf{P}_n(k) = \delta^k (P_{N+1}(0), P_{N+2}(0), \ldots, P_{N+M}(0))' = \delta^k \mathbf{P}_n(0). \tag{39}$$

Define next the $N \times N$ matrix $\mathbf{F}_a$ and the $N \times M$ matrix $\mathbf{F}_n$ with entries

$$F_{ij}^a = \begin{cases} 0, & \text{if } i = j \\ \dfrac{\gamma_i G_{ij}}{G_{ii}}, & \text{if } i \neq j \end{cases} \tag{40}$$

$i \in \{1, 2, 3, \ldots, N\}$, $j \in \{1, 2, 3, \ldots, N\}$, and

$$F_{ij}^n = \frac{\gamma_i G_{ij}}{G_{ii}} \tag{41}$$

$i \in \{1, 2, 3, \ldots, N\}, j \in \{N+1, N+2, N+3, \ldots, N+M\}$ correspondingly. Then, the DPC/ALP updating rule (16) for the powers of the active links can be written

$$\mathbf{P}_a(k+1) = \delta\,(\mathbf{F}_a\mathbf{P}_a(k) + \mathbf{F}_n\mathbf{P}_n(k) + \mathbf{u}_a) \tag{42}$$

where

$$\mathbf{u}_a = \left(\frac{\gamma_1\eta_1}{G_{11}}, \frac{\gamma_2\eta_2}{G_{22}}, \frac{\gamma_3\eta_3}{G_{33}}, \ldots, \frac{\gamma_i\eta_i}{G_{ii}}, \ldots, \frac{\gamma_N\eta_N}{G_{NN}}\right)' \tag{43}$$

is the vector of noise powers (rescaled by γ_is and G_{ii}s of the active links). The first term of the right-hand side of (42) reflects the interference between active links, while the second term reflects the interference of the inactive links on the active ones. Using (39), we can rewrite (42) as

$$\mathbf{P}_a(k+1) = \delta\left(\mathbf{F}_a\mathbf{P}_a(k) + \delta^k\mathbf{F}_n\mathbf{P}_n(0) + \mathbf{u}_a\right). \tag{44}$$

Recursively substituting in (44), we get

$$\mathbf{P}_a(k) = \delta^k\mathbf{F}_a^k\mathbf{P}_a(0) + \delta^k\left[\sum_{i=0}^{k-1}\mathbf{F}_a^i\right]\mathbf{F}_n\mathbf{P}_n(0) + \delta\left[\sum_{i=0}^{k-1}\delta^i\mathbf{F}_a^i\right]\mathbf{u}_a. \tag{45}$$

Dividing by δ^k and taking the limits as $k \to \infty$, we get

$$\lim_{k\to\infty}\left[\frac{\mathbf{P}_a(k)}{\delta^k}\right] = \lim_{k\to\infty}\left[\mathbf{F}_a^k\right]\mathbf{P}_a(0) + \lim_{k\to\infty}\left[\sum_{i=0}^{k-1}\mathbf{F}_a^i\right]\mathbf{F}_n\mathbf{P}_n(0) + \lim_{k\to\infty}\left[\frac{\sum_{i=0}^{k-1}\delta^i\mathbf{F}_a^i}{\delta^{k-1}}\right]\mathbf{u}_a \tag{46}$$

and we need to show that the limits in the right-hand side exist and actually compute them. The first thing to observe is that since all the links in $\mathcal{A}_0 = \{1, 2, 3, \ldots, N\}$ are active (compatible), the Perron–Frobenius eigenvalue of $\mathbf{F}_a$ is less than one (Fact 2.1), therefore

$$\lim_{k\to\infty}\mathbf{F}_a^k = 0 \tag{47}$$

and

$$\lim_{k\to\infty}\left[\sum_{i=0}^{k-1}\mathbf{F}_a^i\right] = \sum_{i=0}^{\infty}\mathbf{F}_a^i = (\mathbf{I}-\mathbf{F}_a)^{-1}. \tag{48}$$

The computation of the third limit of the right-hand side of (46) is more subtle. From (47) we have that for every $\phi > 0$, there is a k_o such that $\mathbf{F}_a^k < [\phi]$ for every $k > k_o$—where $[\phi]$ is the $N \times N$ matrix with all its elements equal to ϕ and the inequality holds componentwise. Then

$$0 \le \lim_{k\to\infty}\frac{\sum_{i=0}^{k-1}\delta^i\mathbf{F}_a^i}{\delta^{k-1}} = \lim_{k\to\infty}\frac{\sum_{i=k_o}^{k-1}\delta^i\mathbf{F}_a^i}{\delta^{k-1}} < \lim_{k\to\infty}\frac{\sum_{i=0}^{k-1}\delta^i[\phi]}{\delta^{k-1}} = \frac{\delta}{\delta-1}[\phi] \tag{49}$$

so letting ϕ relax to zero, we see that the whole term has to be 0.

Using (47)–(49), we finally get from (46)

$$\lim_{k\to\infty}\left[\frac{\mathbf{P}_a(k)}{\delta^k}\right] = (\mathbf{I}-\mathbf{F}_a)^{-1}\mathbf{F}_n\mathbf{P}_n(0) = \mathbf{D}_a^* = (D_1^*, D_2^*, D_3^*, \ldots, D_N^*) < \infty \tag{50}$$

as required. Dividing (42) by δ^{k+1} and letting $k \to \infty$, we get

$$\mathbf{D}_a^* = \mathbf{F}_a\mathbf{D}_a^* + \mathbf{F}_n\mathbf{D}_n^* \tag{51}$$

where actually $\mathbf{D}_n^* = \mathbf{P}_n(0)$. Isolating the ith row, substituting the values of F_{ij}^a, F_{ij}^n, we get

$$D_i^* = \gamma_i\left[\sum_{j\in\{\mathcal{A}_0\cup\mathcal{B}_0\}-i}\frac{G_{ij}}{G_{ii}}D_j^*\right] \tag{52}$$

for every $i \in \{1, 2, 3, \ldots, N\}$.

The SIR of the ith link at the kth power update is given by

$$R_i(k) = \frac{P_i(k)}{\sum_{j\in\{\mathcal{A}_0\cup\mathcal{B}_0\}-i}\frac{G_{ij}}{G_{ii}}P_j(k) + \frac{\eta_i}{G_{ii}}} \tag{53}$$

hence, dividing both the numerator and the denominator by δ^k and letting $k \to \infty$, we get

$$\lim_{k\to\infty}R_i(k) = \frac{D_i^*}{\sum_{j\in\{\mathcal{A}_0\cup\mathcal{B}_0\}-i}\frac{G_{ij}}{G_{ii}}D_j^*} = \gamma_i \tag{54}$$

for every $i \in \{1, 2, 3, \ldots, N\}$, because of (52). This concludes the proof of the proposition. ∎

We can now study the situation where the $\mathcal{B}_0$ links are **fully admissible** to the network, in the sense that there exists a configuration of transmitter powers that satisfies the SIR requirements γ_i of all links in $\mathcal{A}_0 \bigcup \mathcal{B}_0$. That is, there is a positive power vector $\mathbf{P} > 0$ such that $(\mathbf{I}-\mathbf{F})\mathbf{P} \ge \mathbf{u}$, or equivalently (by Fact 2.1)

$$(\mathbf{I}-\mathbf{F})^{-1} \quad \text{exists and has positive entries} \tag{55}$$

where $\mathbf{F}$ and $\mathbf{u}$ are defined as in Section II.

Proposition 5.2 (Fully Admissible Links): If the originally inactive links in $\mathcal{B}_0$ are fully admissible, then there exists a finite time $k_o < \infty$ such that

$$\mathcal{A}_k = \mathcal{A}_0 \bigcup \mathcal{B}_0, \quad \text{for every } k \in \{k_o, k_o+1, k_o+2, \ldots\}. \tag{56}$$

Therefore, if the SIR requirements of all links are compatible, the new ones will also eventually become active, being admitted into the network. This verifies that the algorithm does what it was designed to do.

Proof: Recall that if an inactive link becomes active at some step of the DCP-ALP algorithm, it remains so forever after. Therefore, in order to prove the proposition, it is enough to show that there is a finite time k_1 and some link $i_1 \in \mathcal{B}_0$, such that $\mathcal{A}_{k_1} = \mathcal{A}_0 \bigcup \{i_1\}$; that is, some originally inactive link i_1 becomes active at time k_1. Indeed, we can then restart the process at time k_1 and repeat exactly the same arguments for the now enlarged active set $\mathcal{A}_0 \bigcup \{i_1\}$, and so on…

Arguing by contradiction, suppose that no link in $\mathcal{B}_0$ ever becomes active. Then, from Proposition 5.1 we have that

$$\lim_{k\to\infty}\frac{\mathbf{P}}{\delta^k} = \mathbf{D}^* \tag{57}$$

where $\mathbf{D}^* = \{D_1^*, D_2^*, D_3^*, \ldots, D_N^*, D_{N+1}^*, D_{N+2}^*, \ldots, D_{N+M}^*\}$ and $D_i^* = P_i(0) > 0$ for every $i \in \{N, N+1, \ldots, N+M\}$. Therefore

$$\mathbf{D}^* \quad \text{has at least one positive component.} \tag{58}$$

From Proposition 4.1, we have that for every $k \in \{0, 1, 2, \ldots\}$

$$R_i(k) = \frac{G_{ii}P_i(k)}{\displaystyle\sum_{j\in\{\mathcal{A}_0 \bigcup \mathcal{B}_0\}-i} G_{ij}P_j(k) + \eta_i} \geq \gamma_i \tag{59}$$

for every $i \in \{1, 2, 3, \ldots, N\}$ (active links). Dividing both the numerator and denominator of the fraction by δ^k and taking the limits as $k \to \infty$, we get

$$R_i^* = \frac{G_{ii}D_i^*}{\displaystyle\sum_{j\in\{\mathcal{A}_0 \bigcup \mathcal{B}_0\}-i} G_{ij}D_j^*} = \gamma_i \tag{60}$$

or equivalently

$$D_i^* - \sum_{j\in\{\mathcal{A}_0 \bigcup \mathcal{B}_0\}-i} \frac{\gamma_i G_{ij}}{G_{ii}} D_j^* = v_i = 0 \tag{61}$$

for every $i \in \{1, 2, 3, \ldots, N\}$, because of Proposition 5.1. On the contrary, for every $i \in \{N+1, N+2, \ldots, N+M\}$ (permanently inactive links), we have

$$R_i(k) = \frac{G_{ii}P_i(k)}{\displaystyle\sum_{j\in\{\mathcal{A}_0 \bigcup \mathcal{B}_0\}-i} G_{ij}P_j(k) + \eta_i} \leq \gamma_i \tag{62}$$

and similarly taking the limits, we get

$$R_i^* = \frac{G_{ii}D_i^*}{\displaystyle\sum_{j\in\{\mathcal{A}_0 \bigcup \mathcal{B}_0\}-i} G_{ij}D_j^*} \leq \gamma_i. \tag{63}$$

Equivalently, for $i \in \{N+1, N+2, \ldots, N+M\}$, we have

$$D_i^* - \sum_{j\in\{\mathcal{A}_0 \bigcup \mathcal{B}_0\}-i} \frac{\gamma_i G_{ij}}{G_{ii}} D_j^* = v_i \leq 0. \tag{64}$$

Putting together (61) and (64), we can write

$$(\mathbf{I} - \mathbf{F})\mathbf{D}^* = \mathbf{v} \tag{65}$$

where $\mathbf{v} = (v_1, v_2, \ldots, v_N, v_{N+1}, \ldots, v_{N+M})$ with

$$v_i = \begin{cases} 0, & \text{if } i \in \{1, 2, 3, \ldots, N\$ \\ \leq 0, & \text{if } i \in \{N+1, N+2, \ldots, N+M\}. \end{cases} \tag{66}$$

Due to (55) we have

$$\mathbf{D}^* = (\mathbf{I} - \mathbf{F})^{-1}\mathbf{v}. \tag{67}$$

If $\mathbf{v} = 0$, then we immediately get a contradiction, because $\mathbf{D}^* \neq 0$. Otherwise, in view of (66), there is some $i \in \{N+1, N+2, \ldots, N+M\}$ for which $v_i < 0$. Then, we also get a contradiction, using (58), (55), and (66). This completes the proof of Proposition 5.2. ■

We can now refine our understanding of the case of fully admissible links by considering the following two important subcases, which lead to quite different system behavior. First, suppose that there exists a configuration of transmitter powers such that each link $i \in \mathcal{A}_0 \cup \mathcal{B}_0$ satisfies the enhanced SIR requirement $\delta\gamma_i$. That is, there is a positive power vector $\mathbf{P}_\delta > 0$ such that $(\mathbf{I} - \delta\mathbf{F})\mathbf{P}_\delta \geq \mathbf{u}$, or equivalently (by Fact 2.1)

$$(\mathbf{I} - \delta\mathbf{F})^{-1} \quad \text{exists and has positive entries} \tag{68}$$

where $\mathbf{F}$, $\mathbf{u}$, and δ are defined as in Sections II and IV. We then call the links **δ-compatible**. Note that in the case of fully admissible links studied above, we simply had 1-compatible links. δ-compatibility ($\delta > 1$) naturally implies full admissibility.

Proposition 5.3 (δ-Compatible Links): If the links $\mathcal{A}_0 \bigcup \mathcal{B}_0$ are δ-compatible ($\delta > 1$), then there exists a finite time $k_o < \infty$ such that

$$\mathcal{A}_k = \mathcal{A}_0 \bigcup \mathcal{B}_0, \quad \text{for every } k \in \{k_o, k_o+1, k_o+2, \ldots\}. \tag{69}$$

and all links become active eventually. Moreover

$$\lim_{k\to\infty} \mathbf{P}(k) = (\mathbf{I} - \delta\mathbf{F})^{-1}\mathbf{u} < \infty \tag{70}$$

and

$$\lim_{k\to\infty} R_i(k) = \delta\gamma_i \tag{71}$$

for every $i \in \mathcal{A}_0 \bigcup \mathcal{B}_0$.

Proof: The links being δ-compatible automatically implies that they are fully admissible. Indeed, since $\delta > 1$, (68) supersedes (55). From Proposition 5.2, we see that all links will become active after some finite time k_o; hence, after that time the system will evolve according to the plain DPC algorithm $\mathbf{P}(k+1) = \delta\mathbf{F}\mathbf{P}(k) + \mathbf{u}$. The result follows trivially given the discussions of Sections II and III. ■

Remark 5.1: Note that if the SIR requirements of all links are δ-compatible, not only will all the links eventually become active, but also their SIRs will converge to the raised (enhanced) SIR thresholds $\delta\gamma_i$, while the transmitter powers will remain finite.

Proposition 5.4 (Fully Admissible, Not δ-Compatible Links): If the links $\mathcal{A}_0 \bigcup \mathcal{B}_0$ are fully admissible but not δ-compatible, then there exists a finite time $k_o < \infty$ such that

$$\mathcal{A}_k = \mathcal{A}_0 \bigcup \mathcal{B}_0, \quad \text{for every } k \in \{k_o, k_o+1, k_o+2, \ldots\}. \tag{72}$$

and all inactive links become active eventually. However

$$\lim_{k\to\infty} P_i(k) = \infty \tag{73}$$

for all $i \in \mathcal{A}_0 \bigcup \mathcal{B}_0$. Hence, the transmitter powers diverge to infinity, but all links stay active.

Proof: Since all links are fully admissible, from Proposition 5.2, we have that they will all become active after some finite time k_o. Therefore, for all $k \geq k_o$, the power updates will follow the plain DPC algorithm

$$\mathbf{P}(k+1) = \delta\mathbf{F}\mathbf{P}(k) + \mathbf{u}. \tag{74}$$

However, since the links are not δ-compatible the powers will diverge to infinity. ■

The reason for the divergence of transmitter powers in Proposition 5.4 is this: although the SIRs of all links $i \in \mathcal{A}_0 \bigcup \mathcal{B}_0$ eventually rise above their targets γ_i, they cannot reach the enhanced targets $\delta\gamma_i$ they are shooting for, because the links are not δ-compatible. Having been admitted to the network by exceeding γ, they keep shooting for unattainable targets $\delta\gamma_i$, driving their powers to infinity. We will see in Section VII how to handle this problem. Had the plain DPC algorithm (11) been used, the link SIRs would have converged to their targets γ_i asymptotically (despite intermittent fluctuations below them) and the powers would have remained finite.

Targeting higher SIRs $\delta\gamma$, rather than the minimal acceptable γ, some of the aggregate network capacity (average number of active links in the channel) is traded away for the extra $(\delta - 1)\gamma$ of performance per link. Since δ can be chosen to be very close to 1, the capacity loss can be made arbitrarily small. In any case, any small loss of capacity is overcompensated by the DPC/ALP benefits in overall network performance, like active link protection and others discussed later. Actually, following some relaxation schedule for δ-1 (for example, every 100 DPC/ALP steps, δ-1 drops to half its previous value), enhanced SIR targets $\delta\gamma_i$ can be gradually relaxed to the γ_i ones. Then, the effective network capacity under DPC/ALP grows toward the one under DPC. The relaxation schedule could be globally dispensed by the network over a separate control channel that the links listen to in certain time slots.

VI. The Case of Partially Admissible New Links. DPC/ALP with Voluntary Drop-Out

As DPC/ALP evolves, inactive links see their SIRs rising (not decreasing). In the general case, some new links manage to become active, while the rest never gain admission (their SIRs simply saturate below γ). This is because the SIR targets of all links may not be simultaneously satisfied. It might then be overall beneficial that some of the latter links drop out and try for admission later. We explore this situation below, starting with a demonstrative simulation of a simple case which highlights the underlying intuition.

Figs. 1 and 2 show the evolution of the SIRs of four uplinks of a simple four-cell network, over iterations of the DCP/ALP algorithm, when the SIR target γ is set first at 14 dB which is achievable (Fig. 1) and then at 18 dB which is not (Fig. 2). The initial SIRs (powers) are arbitrarily chosen. In the first case, the DPC/ALP algorithm activates eventually every initially inactive link, and the SIRs converge to $\delta\gamma = 15$ dB (as expected). In the second case, where the target SIR is not achievable by all links simultaneously, the DPC/ALP algorithm exhibits the following behavior.

1) It maintains the SIR of every initially active link above its required threshold.
2) It suppresses/saturates the SIR of every initially inactive link which fails to rise above its SIR target to become active, in this case, links 3 and 4.
3) After two consecutive iterations where the SIR of link 3 fails to improve by at least 0.1 dB (for 1 dB increase in power), the link concludes that the channel is congested and drops out of the channel voluntarily.

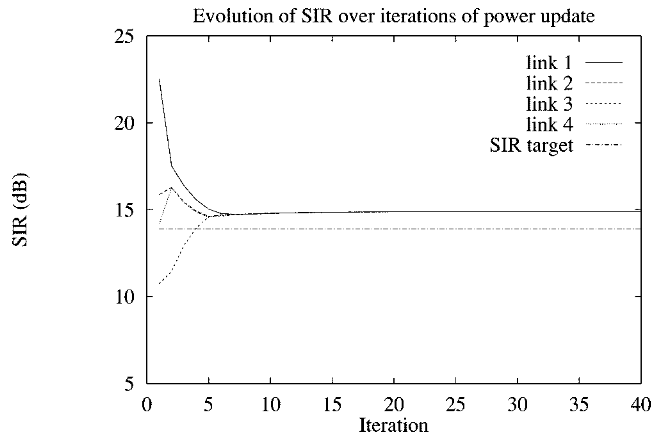

Fig. 1. SIR evolution of the four mobile-to-base links under DPC/ALP with SIR requirements $\gamma = 14$ dB achievable by all links. Simulated base station receivers are located on a square at X/Y positions (100 100), (100,-100), (-100,100), ($-100, -100$) (in meters). Mobiles (transmitters) are located at positions (131 173), (204,-81), (217 171), (210,93) correspondingly. Power gain decreases proportionally to the inverse fourth power of distance. All target SIRs are equal. $\delta = 1.26$ (approx. 1 dB). The SIR scales is logarithmic and the units are dB.

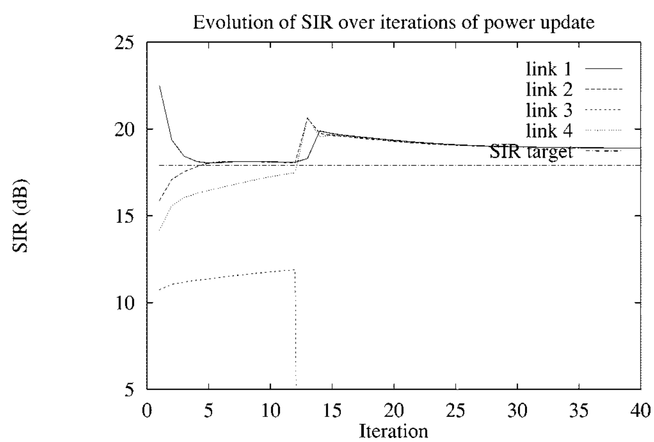

Fig. 2. SIR evolution with SIR targets raised to $\gamma = 18$ dB which is not achievable by all four links simultaneously; the lowest dropping out allows another to gain admission. The rest of the simulation parameters are as in Fig. 1.

4) The dropping-out of link 3 reduces interference in the channel and allows link 4 to become active!

The previous simulated example indicates that the initial DPC/ALP algorithm (15), (16) should be modified to allow for new links to drop out (drop their power to zero) voluntarily, when sensing that the channel is congested and realizing that they have a remote chance of becoming active. A link that drops out of the channel may immediately try to access another network channel (if there is one) or even the same after a while. In the latter case, it should remain dormant during a back-off period and then start powering up again from the beginning. Depending on the criterion used for dropping out, we can design different algorithms. Two of them are presented below, representing two diverse approaches.

A. Time-Out-Based Voluntary Drop-Out (VDO)

The first approach is based on the idea of a *time-out*, when a new link attempts to gain admission to the network and does not succeed for a while. Its key points are the following. All links update their powers according to the DPC/ALP algorithm (15), (16). A new link i initially sets a target time span T_i for achieving admission and tries to become active within it. If it is not successful by time T_i, then it computes a drop-out horizon D_i (as a decreasing function of the distance of its current SIR from its target one γ_i) and continues to compete for admission until time $(T_i + D_i)$. If it has still not been admitted by time $(T_i + D_i)$, it drops out voluntarily, setting its power to 0. It may re-initiate an admission attempt later in the same or another channel. The elimination of the link reduces the interference on other ones competing for admission in the channel and raises their chances of success. The algorithm is specified as follows:

Algorithm 2—DPC/ALP/VDO with Adaptive Time-Out: During the kth time slot the transmission power of each link is updated according to the following process.

1) Link i measures its current SIR and determines whether it is active ($R_i(k) \geq \gamma_i$ and $i \in \mathcal{A}_k$) or inactive ($R_i(k) < \gamma_i$ and $i \in \mathcal{B}_k$). If active, it goes to step 2a; otherwise, to step 3a).

2)

a) If $k \in \{K_i^a, K_i^a+1, K_i^a+2, \ldots, K_i^a+S_i\}$, active link i updates its power according to DPC/ALP (15), sets $k \leftarrow k+1$ and goes to step 1. K_i^a is the first time that link i becomes active and S_i its service time (duration of communication).

b) If $k = K_i^a + S_i + 1$, link i "dies" naturally, setting its power to zero and removing itself from the set of active links $\mathcal{A}_k \leftarrow \mathcal{A}_k - \{i\}$, having completed its required communication.

3)

a) If $k \in \{K_i^o, K_i^o+1, K_i^o+2, \ldots, K_i^o+T_i+D_i-1\}$, the inactive link i updates its power according to DPC/ALP (15), sets $k \leftarrow k+1$ and goes to step 1. K_i^o is the time slot when link i started its most recent admission trial. T_i is the initial admission horizon. D_i is the drop-out horizon, computed at time $K_i^o + T_i$ according to the formula

$$D_i = f_i\left(\gamma_i - R_i(T_i)\right) = \lfloor A_i e^{-\alpha_i(\gamma_i - R_i(T_i))} \rfloor \quad (75)$$

where $A_i, \alpha_i \geq 0$ and $\lfloor\,\rfloor$ denotes the lower integer part of its argument. The function $f_i(\,)$ is decreasing in its argument, capturing the intuition that the closer link i finds itself to its target γ_i at time T_i [the smaller the $\Delta R_i(T_i) = \gamma_i - R_i(T_i)$], the longer it should try before dropping out.

b) If $k = K_i^o + T_i + D_i$, link i voluntarily drops out (sets its power to zero and removes itself from the set of inactive links $\mathcal{B}_k \leftarrow \mathcal{B}_k - \{i\}$), sets the back-off timer $K_i^b \leftarrow k = K_i^o + T_i + D_i$, sets $k \leftarrow k+1$ and goes to step 4a.

4)

a) If $k \in \{K_i^b, K_i^b+1, \ldots, K_i^b+B_i\}$, link i remains dormant in the back-off state (keeping its power to zero), sets $k \leftarrow k+1$ and cycles back to step 4a. B_i is the length of the back-off period, that is, the time the link stays dormant.

b) If $k = K_i^b + B_i + 1$, the link wakes up setting its power to P_o (initial power, see Section VIII), sets $K_i^o \leftarrow k$, sets $k \leftarrow k+1$ and goes to step 1.

The admission and drop-out horizons could also taken to be probabilistic, T_i and D_i being interpreted as expected times, for example, they could be drawn from a geometric distributions of rates $1/T_i$, $1/D_i$ correspondingly. They could be easily implemented by independent coin tossing.

The admission T_i and the drop-out D_i horizons are design parameters of the system to be optimized by testing. Indeed, too short a time-out will cause the link to drop out (possibly) unnecessarily, while too long a time-out will result in the link congesting the channel for too long before dropping out. The system behavior as a function of these two parameters is studied by simulation in Section IX.

B. SIR-Saturation-Based Voluntary Drop-Out

Algorithm 3 below is based on Proposition 4.3 and has a different approach than Algorithm 2, regarding the drop-out of unsuccessful links.

The key points of the algorithm are the following. All links update their powers according to the plain DPC/ALP algorithm (15). Each new link i keeps trying to become active as long as it observes some adequate SIR improvement over a recent memory window of length M_i. If persistently (for more than M_i steps) no such improvement occurs, link i starts flipping a coin to decide whether to drop out in the following step or not. Coin flips are independent of each other and the drop-out probability is a decreasing function of the difference between the current SIR of the link and its target one.

As explained in the previous sections (Proposition 4.3), if the channel is congested and link i is not admissible, its SIR will saturated below its target value. Consecutive power increases will not bring about any significant SIR improvement. The link will therefore sense high congestion and initiate a randomized drop-out process. If some other link drops out sooner, the one under consideration may experience some significant SIR improvement, which will renew the process and give it a stronger chance of ending successfully.

Algorithm 3—DPC/ALP/VDO with SIR-Saturation-Based Drop-Out: This algorithm is exactly the same as Algorithm 2, except for step 3 which implements a different drop-out criterion. The latter is as follows:

3)

a) If $R_i(m) - R_i(m-1) \geq r_i$ for some $m \in \{k-M_i, k-M_i+1, \ldots, k-1, k\}$, the inactive link i updates its power according to DPC/ALP (15), sets $k \leftarrow k+1$ and goes to step 1. M_i is the memory window in which the link must have observed instantaneously some significant SIR improvement $R_i(m) - R_i(m-1)$, larger than some lower threshold r_i.

b) If $R_i(m) - R_i(m-1) < r_i$ for every $m \in \{k - M_i, k - M_i + 1, \ldots, k-1, k\}$, the inactive link i computes a drop out probability

$$\mathcal{P}_i^{\text{drop}}(k) = h_i(\gamma_i - R_i(k)) = 1 - e^{-\beta_i(\gamma_i - R_i(k))} \quad (76)$$

where $\beta_i \geq 0$, and flips an independent (from previous events) coin so that:

i) with probability $(1 - \mathcal{P}_i^{\text{drop}}(k))$ the link does *not* drop out, updates its power according to DPC/ALP (15), sets $k \leftarrow k+1$ and goes to step 1.

ii) with probability $\mathcal{P}_i^{\text{drop}}(k)$, the link voluntarily drops out, (setting its power to 0 and removing itself from the set of inactive links $\mathcal{B}_k \leftarrow \mathcal{B}_k - \{i\}$), sets the back-off timer $K_i^b \leftarrow k$, sets $k \leftarrow k+1$ and goes to step 4a.

Therefore, if link i has not observed any significant SIR improvement during the last M_i steps, it drops out with probability $\mathcal{P}^{\text{drop}}$. The closer the link is to its target γ_i the smaller its tendency to drop out should be, hence, $\mathcal{P}_i^{\text{drop}}(k) = h_i(\Delta R_i(k)) = h_i(\gamma_i - R_i(k))$, where $h_i(\,)$ is increasing; a simple choice is $1 - e^{-\beta_i \Delta R_i(T_i)}$, used in Algorithm 3. The parameters M_i, r_i, $\mathcal{P}_i^{\text{drop}}$ can be further chosen to optimize the performance of the system.

VII. DPC/ALP with Constrained Transmitter Powers—Forced Drop-Out (FDO)

As increasingly more links are admitted to the network and congestion builds up, the Pareto-optimal power vector P^* increases in all components and the Perron–Frobenius eigenvalue ρ_F is pushed closer to 1. What if the power of link i cannot exceed some maximum threshold $P_i^{\max}$ due to design limitations? In particular, as new links power up in a congested neighborhood of the network, some active one i may need to attain power values beyond $P_i^{\max}$ in order to remain active. If it cannot, it will see its SIR drop below γ_i and become inactive. To prevent that from happening we equip the link admission process with a forced drop-out (FDO) mechanism which causes new/inactive links to drop out when they push active ones beyond their maximum powers. When an active link is about to exceed its power limit, it transmits a *distress signal* (special tone in a control slot or some separate control channel) at a certain power level which is received by links in its vicinity. All *inactive* links which hear the distress signal above a certain power threshold drop out automatically, decongesting the neighborhood of the active link in distress and allowing it to relax its power and remain active. Note that due to the bounded power overshoot property of DPC/ALP [$P_i(k+1) \leq \delta P_i(k)$ for every k], the ith link's power $P_i(k)$ has to visit (cross) the interval $\Delta P_i^{\max} = [P_i^{\max}/\delta, P_i^{\max}]$ before potentially exiting into the forbidden region $(P_i^{\max}, \infty)$. This nice property is not true for the plain DPC. The distress signal is transmitted by link i when $P_i(k) \in \Delta P_i^{\max}$ or the link visits the alert zone $\Delta P_i^{\max}$. That zone is rather slim (since δ is slightly larger than 1 in practice), so false alarms are unlikely to occur. Needless to say, if some limited interlink communication is allowed via some logical control channel, the particular incoming link responsible for the situation can be easily uniquely identified and killed by an "interrupt signal" on the control channel.

The FDO mechanism needs to be invoked also in the special situation described in Proposition 5.4 of fully admissible but not δ-compatible links. If this occurs and a new link becomes active without being δ-compatible, all powers will start blowing up to infinity. The first link to hit its maximum power limit will transmit the distress signal. The latter will appear very soon after the time that the last link became active and triggered this sequence of events, due to the exponential speed of power explosion. Therefore, after a new link becomes active it should wait for a short time horizon to see if a distress signal will appear soon. If so, it should drop out. If not, beyond that horizon it can consider itself permanently admitted and active in the channel. This aberrant situation is theoretically possible, but would be rather rare in practice, for the following reason. Intuitively, one can observe that, since δ is slightly larger than 1, the situation can primarily occur under high congestion when the link powers are already close to their maxima. In a dynamic environment of several new links fighting for admission, the most likely case is that FDO will be triggered by a totally inadmissible link and the local hotspot will immediately be diffused completely. Of course, if some interlink communication is allowed, the scenario of Proposition 5.4 can be eliminated in several obvious ways. We do not elaborate further, as we are mostly interested in the fully distributed case.

VIII. Initiation of the Link Admission Process—Initial Power Issue

When new links initiate their admission process, they start by setting their power at P_o to join the set of inactive links $\mathcal{B}$. A new link which suddenly powers up to P_o may interfere strongly enough with some unsuspecting active link i to cause the SIR of the latter to temporarily drop below γ_i. This is a situation we would like to avoid. The problem here is the sudden and uncoordinated appearance of the new user which is unknown to the existing ones. In order for no active link to be adversely affected P_o must be small enough, depending on the particular networking scenario. For example, as simple calculations show, with $P_o \leq ((\delta - 1)\eta)/G_{\max}$ no active link will drop below its SIR threshold γ_i upon appearance of a new one, given that all active links have stabilized at their enhanced SIR values $\delta\gamma_i$ and $G_{\max}$ is the maximum power gain (interaction strength) between the new link powering up and all active ones.

Another practical approach is to have active links rapidly recover from instantaneous dippings of their SIRs below γ (becoming inactive for a moment due to some new one powering up to P_o). The question is what power updating rule should be followed by an already active link if/when it becomes inactive for a time slot. It should keep updating its power as an active link, despite the fact that it is "technically inactive" in the particular time slot. We call this rule "once active, always update as active." Note that due to the fast geometric convergence of the DPC algorithm the SIR of the link under consideration will rapidly shoot up to $\delta\gamma$, crossing the threshold γ and becoming again active fast.

A combination of a low enough initial power P_o and a rule of the type "once active, always update as active" could be employed. Of course, the practical question is how often does it happen that a new link powering up from P_o drags an active one below its γ. In the simulation experiments presented in Section IX, we see that this is very rare even under heavy traffic loads (see footnote 3).

IX. Dynamical Effects and Performance Aspects of DPC/ALP with VDO/FDO

We have run extensive simulation experiments to investigate the network dynamics under the DPC/ALP algorithm with VDO/FDO. Their primary purpose has been the identification and investigation of *general dynamical effects* dominating the network behavior. The simulated network is a collection of randomly placed links with spatially uniform statistics. In implementing the VDO process, we employ the adaptive time-out (instead of SIR saturation) mechanism because it allows us to control more parameters (especially T) to excite the network dynamics and study them.

A. Simulation Design

The simulation experiments[1] are designed as follows. Let l.u. be the length unit, p.u. the power unit, and t.u. the time unit (duration of a time slot). We shall attach metric values to the units later, when we consider some specific networking scenarios. The wireless network is assumed to span a square region of side 500 l.u. Calls (links) are generated (arrive) according to a Bernoulli process of arrival rate density λ_d in the range 10^{-7} to 10^{-6} arrivals/(t.u. $\times$ l.u.^{2}) (total arrival rate 25×10^{-3} to 25×10^{-2} arrivals/t.u.). In order to generate a *spatially uniform* statistical mixture of links, each one is randomly constructed as follows. Upon call arrival the link transmitter is uniformly placed in the square region 500×500 l.u.^{2}. The link receiver is placed isotropically around its transmitter (given a reference direction, the link angle is distributed in $[0, 2\pi)$ uniformly) and at a random distance from it. The latter is drawn from a Gaussian distribution with mean 10 l.u. and standard deviation 2 l.u. (negative draws are interpreted as reverse link directions). Links are warped around boundary effects to eliminate boundary effects. The power attenuation is taken to follow the inverse fourth power law

$$G_{ij} = \frac{g}{r_{ij}^4} \tag{77}$$

to account for shadowing and multipath fading in urban environments. Hence, the SIR of the ith transmitter is computed by

$$R_i = \frac{\dfrac{P_i}{r_{ii}^4}}{\displaystyle\sum_{j \neq i} \frac{P_i}{r_{ii}^4} + \frac{\eta_i}{g}} \tag{78}$$

where r_{ij} is the distance (in l.u.) between the transmitter of the jth link and the receiver of the ith one. The normalized noise floor n_i/g is taken to be the same for all receivers and equal to 10^{-9} p.u./l.u.^{4}.

All links have the same SIR target $\gamma = 5$, which may be low for certain applications. We have chosen this low-end SIR in order to have a reasonably high density of active links in equilibrium. This is essential in order to achieve enough spatial statistical mixing for high statistical reliability[2] versus run time of the simulation. Finally, the SIR enhancement factor in the DPC/ALP algorithm is taken to be $\delta = 1.1$; hence, we have a $\epsilon = \delta - 1 = 10\%$ SIR protection margin.

To implement the VDO mechanism, we use Algorithm 2 with the *adaptive time-out* process. The parameters are identical for all links and are described for a representative link below. Upon arrival, say at time t_o, the link seeks admission to the channel for $T = 25$ t.u. If it is not successful in $[t_o, t_o + T]$, it computes the drop-out horizon

$$D = \lfloor A e^{-\alpha(\gamma - R_i(t_o+T))} \rfloor = \lfloor A (e^{-\alpha})^{(\gamma - R_i(t_o+T))} \rfloor \tag{79}$$

using $A = 50$ t.u. and $\alpha = 0.23$ ($e^{-0.23} \approx 0.8$). If the link does not gain admission within the drop-out horizon in $[t_o + T, t_o + T + D]$, it drops out (backs off) and lies dormant for a geometrically distributed time B with mean $\overline{B} = 100$ t.u. (average back-off time). At time $t_o + T + D + B$, the link re-initiates the time-out-based admission process to the channel. The whole process is repeated until the link gains admission, after which it transmits for a geometrically distributed time S with mean $\overline{S} = 1000$ t.u. (mean service time, average call duration), before leaving the network for good. The initial power[3] at which each link starts powering up is $P_0 = 10^{-5}$ p.u.

[1] *Simulation Logistics:* For each point of the performance curves presented later, long simulation runs (mostly of 10^9 t.u. or time slots) have been performed on multiple computer workstations, using time-average estimators. To filter out transient effects and capture earlier the stationary dynamics of the network, the initial 5% of the collected data have been discarded. The random number generator employed used the linear congruential algorithm with 48-bit integer arithmetic (drand48) to generate double-precision floating point values [uniformly distributed in [0,1)] and provide high statistical reliability. The average network size is of the order of 100s of active plus inactive links.

[2] As seen later in Section IX-B, the average number of active links in the network is 100–150 (in the range of parameters we are interested in), or one active link per 2500 l.u. to 1 per 1500 l.u., approximately. From pilot studies that preceded the main simulation, we saw that for higher γs (10–20) the active link density drops significantly, depleting the spatial link sample of the system in stationarity, and adversely affecting the reliability and speed of the simulation.

[3] *The Initial Power Issue:* In the (infrequent) event that the sudden power-up of a new link causes an active link to become temporarily inactive in the simulation, the latter keeps updating its power as an active link and very soon becomes active again. This is actually the situation discussed in Section VIII. If we impose upper bounds on the power gains G_{ij}, or lower bounds on the distance on how close links could be positioned, the previous situation can be fully suppressed; however, that would further complicate the simulation code. Instead, we have treated this as a rare event in the simulation dynamics. Indeed, even under very heavy loading (98% to critical capacity) the average distance between two links in the network is about 3 times the mean link length of a link (10 l.u.) in our simulation—hence, they are rather sparce. Moreover, the average power of active links is of the order or 10^{-1} p.u. (versus an initial power of 10^{-5} for new ones) under these load conditions in the simulation. These observations indicate that there is enough *distance and power protection* between active and new links, so that the aforementioned situation occurs rarely. Higher traffic loads, where it may occur more frequently, are impractical since the delay becomes excessive.

To implement the FDO process we use a power ceiling $P^{\max} = 1$ p.u. for each transmitter. When the power of an active link is in danger of exceeding $P^{\max}$, the link sends a distress signal and all nonactive links in a radius of $L = 100$ l.u. from the transmitter drop out (back off).

The values of the parameters (in l.u., t.u., p.u.) specified above correspond to a standard (reference) operating point[4] of the system. Our intention is to study the system behavior with respect to variations of individual parameters around that operating point. Therefore, parameter values that are redefined below supersede the values set above.

Remark 9.1 (Sample Networking Scenarios): Assigning specific metric values to the units, we can cover several wireless networking scenarios[5] of interest. For example, assume that 1 l.u. = 1 m, 1 t.u. = 10 ms (time slot), and 1 p.u. = 1 W. Then the network spans an area of 0.25 km^2. This could possibly be the case for a network of laptop computers in an ***ad-hoc* networking** scenario. The mean length of each link is 10 m (with 2 m standard deviation). The range of network-wide arrival rate is 2.5–25 arrivals/s. The average call duration is $\overline{S} = 10$ s, while the drop-out process is implemented with $T = 0.25$ s, $A = 0.5$ s, and mean back-off time $\overline{B} = 1$ s. The normalized noise floor is $\eta/g = 1$ nW/m^4, the start-up power $P_0 = 10$ μW, and the maximum power $P^{\max} = 1$ W. Now, let us scale the length unit up by 10 (1 l.u. = 10 m), while leaving the rest as above (1 t.u. = 10 ms, 1 p.u. = 1 W). The simulated network now spans 25 km^2, while the mean link length is 100 m. This could possibly be the case in an **urban cellular** wireless network scenario. The values of all time and power related parameters remain the same, except for the normalized noise floor which must match the space rescaling by becoming $\eta/g = 10^{-9}$ p.u./l.u.^{4} = 10^{-4} nW/m^4.

B. Dynamical Effects and Network Performance

Figs. 3–11 show key performance curves of the network operating under the DPC/ALP algorithm with time-out-based plain VDO (Figs. 3–8) and joint VDO and FDO (Figs. 9–11). Some observed dynamical effects are briefly discussed below.

The significance of VDO for managing congestion is highlighted in Fig. 3, where approximately a 20-fold increase in network capacity (maximal throughput) is observed under VDO over the case where no drop-out is allowed. Note that as the traffic load increases, the network eventually goes unstable by a reinforced "clogging effect." That is, the more inactive links accumulate in the network, the more links try to power up and the higher the interference becomes, making it more difficult for new links to gain admission and forcing them to further accumulate in the network, leading eventually to backlog explosion.

The dependence of admission delay on T is shown in Fig. 4. T is basically a measure of how aggressively a new link seeks admission or how long it tries before dropping out. An explosion of admission delay (and backlog) is observed for low Ts due a "premature drop-out effect." That is, the links do not try long enough before dropping out and retrying, hence, they accumulate in the network and increase the background interference.

Fig. 5 shows the number of active/inactive links in equilibrium as a function of network load, which reaches about 160 active links (and 100 inactive) close to the critical loading. That

[4]The choice of simulation parameters has been mainly motivated by the need to increase the reliability and resolution of the experiments and obtain better understanding of fundamental network dynamics, rather than to match a particular networking scenario.

[5]The simulation results remain invariant under rescalings of time and/or power (because of the definition of R_i); however, a rescaling of space needs to be matched by an analogous rescaling of power (because of the definition of G_{ij}) in order for the simulation results to remain the same.

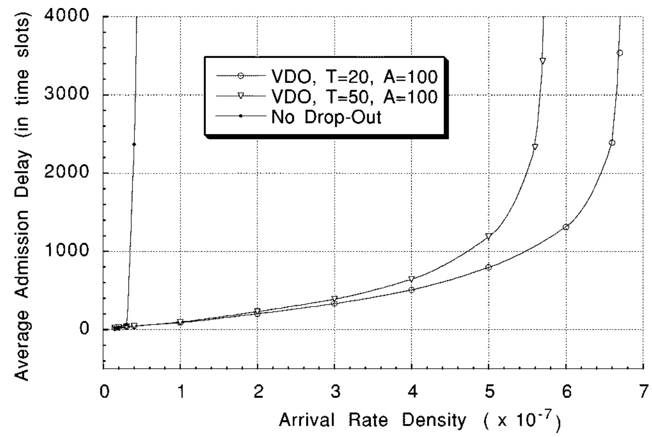

Fig. 3. Average admission delay of a call (link) as a function of the arrival rate density λ_d (traffic) for VDO with $T = 20$ t.u., $A = 100$ t.u., VDO with $T = 50$ t.u., $A = 100$ t.u., and no drop-out.

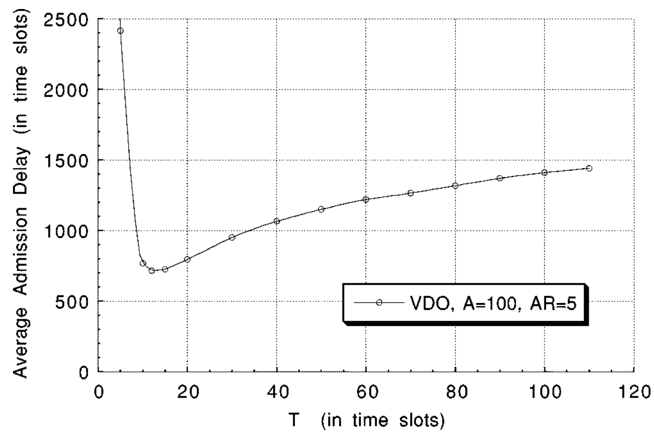

Fig. 4. Dependence of average admission delay on T for VDO with $A = 100$ t.u. at fixed arrival rate (AR) density $\lambda_d = 5 \times 10^{-7}$ arrivals/(t.u. × l.u.^{2}).

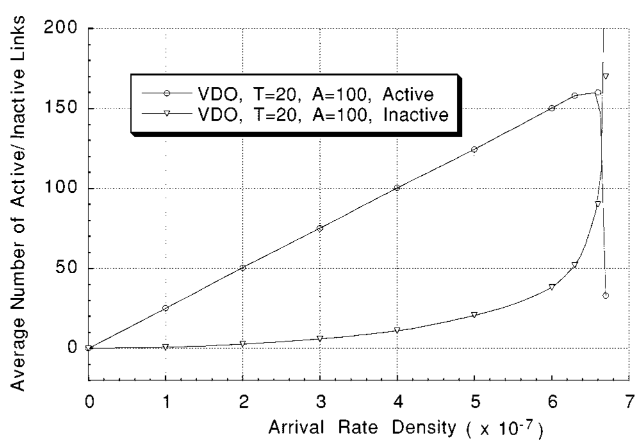

Fig. 5. Average number of active/inactive networks links in stationarity versus traffic λ_d for VDO with $T = 20$ t.u., $A = 100$ t.u.

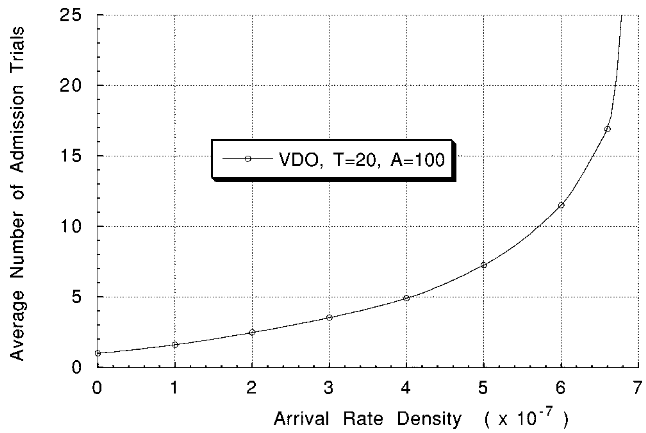

Fig. 6. Average number of admission trials of incoming call/link before gaining admission versus traffic λ_d for VDO with $T = 20$ t.u., $A = 100$ t.u.

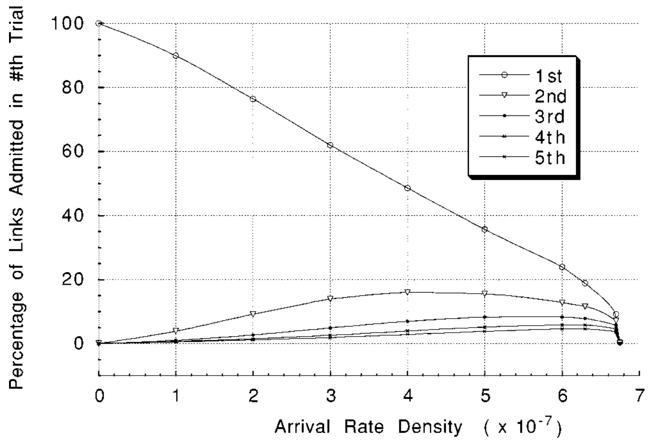

Fig. 7. Percentage of new links (incoming calls) admitted in their 1st, 2nd, 3rd, 4th, and 5th attempt versus traffic λ_d for VDO with $T = 20$ t.u., $A = 100$ t.u.

corresponds to about 1 per 1500 l.u.^{2} on average, so the *average distance of active links* is of the order $\sqrt{1500} \approx 38$ l.u., or 4 times the mean link length. The linear form of the graph is explained as follows. Since the call (link) durations are i.i.d. geometric random variables with mean $\overline{S} = 1000$ t.u., the link departure rate must be $\overline{N}/\overline{S}$, where $\overline{N}$ is the number of active links in stationarity. For input–output flow balance in equilibrium, the active link population should be proportional to λ_d.

Figs. 6 and 7 show the average number of admission trials and drop-out cycles that arriving links have to go through before gaining admission. Finally, in Fig. 8 we see the average admission delay as a function of the mean back-off time $\overline{B}$ of a link after dropping out. An explosion of the average delay occurs for low $\overline{B}$s because dormant links reappear in the network too soon after they drop out, raising the background interference and making it more difficult for inactive ones that did not drop out to gain admission.

An interesting question is how the FDO mechanism affects the overall network performance, besides protecting active links under finite maximum power. As Fig. 9 indicates, joint VDO/FDO can enhance the performance of plain VDO, achieving lower delay and higher throughput. The reason is that FDO tends to "diffuse hotspots" in the network by causing stressful links to drop out.

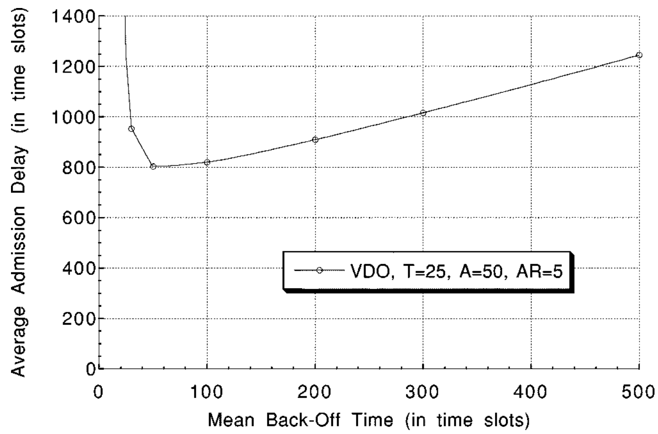

Fig. 8. Average admission delay versus mean back-off time $\overline{B}$ for VDO with $T = 25$ t.u., $A = 50$ t.u. at fixed arrival rate (AR) density $\lambda_d = 5 \times 10^{-7}$ arrivals/(t.u. $\times$ l.u.^{2}).

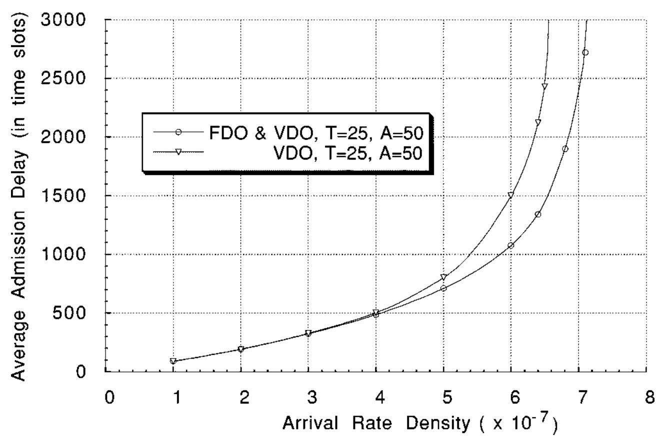

Fig. 9. Average admission delay versus arrival rate density λ_d (traffic load) for joint FDO and VDO with $T = 25$ t.u., $A = 50$ t.u., and only VDO with $T = 25$ t.u., $A = 50$ t.u. with no FDO.

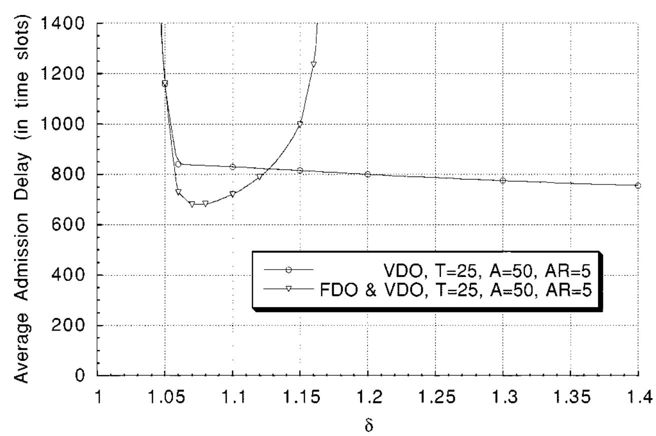

Fig. 10. Average admission delay versus δ at fixed traffic load (AR) $\lambda_d = 5 \times 10^{-7}$ arrivals/(t.u. $\times$ l.u.^{2}) for joint FDO and VDO with $T = 25$ t.u., $A = 50$ t.u., and only VDO with $T = 25$ t.u., $A = 50$ t.u. with no FDO.

The effect of the SIR enhancement factor δ (protection margin $\epsilon = \delta - 1$) on network dynamics and performance is shown in Fig. 10. When δ is very close to 1, the admission delay explodes because inactive links power up too slowly, so in $T + D$ steps they have made very little progress toward gaining admission and drop-out prematurely. Under joint FDO and

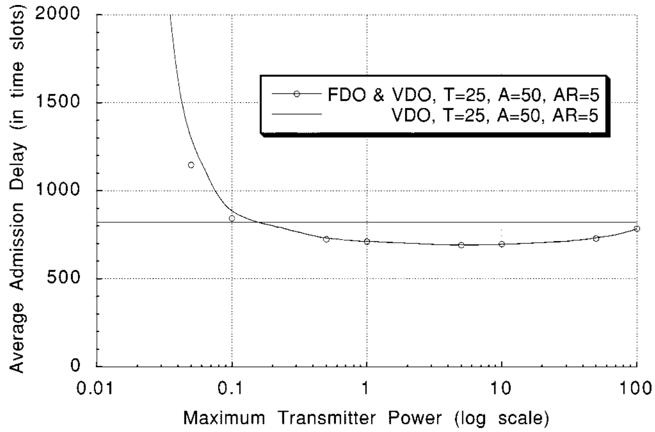

Fig. 11. Average admission delay versus the maximum transmitter power $P^{\max}$ (in logarithmic scale of p.u.) at fixed traffic load (AR) $\lambda_d = 5 \times 10^{-7}$ arrivals/(t.u. × l.u.^{2}) for the case of joint FDO and VDO with $T = 25$ t.u. and $A = 50$ t.u.

VDO, high δs result in high SIR targets $\delta\gamma$ and high transmitter powers, causing frequent hits of the power ceiling $P^{\max}$ (fixed) and forced drop-outs. Note that for a substantial range of δs the joint VDO/FDO process achieves superior performance (lower delay) than the plain VDO one [$\delta \in (1.06, 1.125)$ in this example].

Finally, Fig. 11 shows how admission delay depends on $P^{\max}$. For low power ceilings the admission delay explodes because forced drop-outs become too frequent, increasing the feedback traffic and clogging the system up.

X. Conclusion

A baseline model of wireless networking has been studied, capturing essential dynamics of power control. We have seen that the DPC/ALP/VDO/FDO suite of algorithms allows fully distributed/autonomous joint power and admission control supporting *active link protection.* The key general idea introduced and leveraged here is using a *protection margin* (matched with gradual power-up) in the dynamics of the SIR. This is analogous to the ubiquitous "safety margin concept" in engineering design. It can also prove useful in handling mobility and random propagation effects by "cushioning" the network dynamics during unpredictable events and providing enough time for the power control mechanism to react appropriately.

There are several issues of further research we are currently investigating, as well as implementational ones. First, those of mobility and handoff control, using the protection margin idea mentioned above. Second, how to adaptively choose δ. This should be larger when the network is uncongested, so that links power up fast, and grow smaller as congestion builds up to have links power up more gently. Finally, we are studying the multiple channel case, where a link can choose one among several orthogonal channels to access the network. An important idea is for a link to "differentially probe" a channel to predict at what power it can be admitted to it (if at all). By probing a few channels, it can select the one where it is admissible at the lowest power. A channel probing method and some preliminary encouraging results have been reported in [29]. The latter line of research is currently pursued as an important additional element of power control algorithm design.

Acknowledgment

The authors would like to thank the anonymous referees for providing comments that have considerably improved this paper.

References

[1] J. M. Aein, "Power balancing in systems employing frequency reuse," *COMSAT Tech. Rev.*, pp. 277–299, 1973.
[2] H. Alavi and R. W. Nettleton, "Downstream power control for a spread spectrum cellular mobile radio system," in *Proc. IEEE GLOBECOMM'82*, pp. 84–88.
[3] J. Zander, "Distributed cochannel interference control in cellular radio systems," *IEEE Tran. Veh. Tech.*, vol. 41, pp. 305–311, Mar. 1992.
[4] S. Grandhi, R. Vijayan, and D. J. Goodman, "A distributed algorithm for power control in cellular radio systems," in *Proc. 30th Allerton Conf.*, Monticello, IL, 1992.
[5] S. C. Chen, N. Bambos, and G. J. Pottie, "Admission control schemes for wireless communication networks with adjustable transmitter powers," in *Proc. IEEE INFOCOM'94*, Toronto, Canada.
[6] ——, "On distributed power control for radio networks," in *Proc. ICC'94*, New Orleans, LA.
[7] G. J. Foschini and Z. Miljanic, "A simple distributed autonomous power control algorithm and its convergence," *IEEE Trans. Veh. Tech.*, vol. 42, pp. 641–646, Apr. 1993.
[8] ——, "Distributed autonomous wireless channel assignment with power control," Preprint.
[9] S. C. Chen, N. Bambos, and G. J. Pottie, "On power control with active link quality protection in wireless communication networks," presented at the Princeton Conf. Inform. Syst., Princeton Univ., Princeton, NJ, Mar. 1994.
[10] N. Bambos, S. C. Chen, and G. J. Pottie, "Radio link admission algorithms for wireless networks with power control and active link quality protection," in *Proc. IEEE INFOCOM'95*, Boston, MA, 1995.
[11] D. Mitra, "An asynchronous distributed algorithm for power control in cellular radio systems," in *Proc. 4th WINLAB Workshop*, Rutgers University, New Brunswick, NJ, 1993.
[12] D. Mitra and A. Morrison, "A distributed power control algorithm for bursty transmissions in cellular, spread spectrum wireless networks," in *Proc. 5th WINLAB Workshop*, Rutgers University, New Brunswick, NJ, 1995.
[13] ——, "A novel distributed power control algorithm for classes of service in cellular CDMA networks," Preprint.
[14] N. Bambos and G. J. Pottie, "On power control in high capacity cellular radio networks," in *Proc. IEEE GLOBECOMM'92*, vol. 2, pp. 863–867.
[15] M. Andersin, Z. Rosberg, and J. Zander, "Gradual removals in cellular PCS with constrained power control and noise," *Wireless Networks*, vol. 2, no. 1, pp. 27–43, 1996.
[16] ——, "Distributed discrete power control in cellular PCS," Royal Institute of Technology, Sweden, Tech. Rep. TRITA-IT R 94-23, 1994.
[17] ——, "Soft and safe admission control in cellular networks," *IEEE/ACM Trans. Networking*, vol. 5, pp. 255–265, Apr. 1997.
[18] M. Andersin, "Power control and admission control in cellular radio systems," Ph.D. dissertation, Royal Institute of Technology, Sweden, 1996.
[19] E. Seneta, *Non-Negative Matrices*. London, U.K.: G. Allen, 1973.
[20] M. B. Pursley, "The role of spread spectrum in packet radio networks," *Proc. IEEE*, vol. 75, Jan. 1987.
[21] N. Bambos, "Toward power-sensitive network architectures in wireless communications: Concepts, issues and design aspects," *IEEE Personal Commun. Mag.*, vol. 5, pp. 50–59, Mar. 1998.
[22] F. R. Gantmacher, *The Theory of Matrices*. New York, NY: Chelsea, 1971.
[23] S. Hanly, "Capacity and power control in a spread spectrum macro diversity radio networks," *IEEE Trans. Commun.*, vol. 44, pp. 247–256, Feb. 1996.
[24] ——, "An algorithm for combined cell-site selection and power control to maximize cellular spread spectrum capacity," *IEEE J. Select. Areas Commun.*, vol. 13, pp. 1332–1340, July 1995.
[25] R. Yates and C. Y. Huang, "Integrated power control and base station assignment," *IEEE Trans. Veh. Technol.*, vol. 44, pp. 638–644, Mar. 1995.
[26] ——, "Constrained power control and base station assignment in cellular radio systems," Preprint.

[27] R. Yates, "A framework for uplink power control in cellular radio systems," *IEEE J. Select. Areas Commun.*, vol. 13, pp. 1341–1347, July 1995.
[28] S. Grandhi, R. Yates, and J. Zander, "Constrained Power Control," *Wireless Commun.*, vol. 2, no. 3, Aug. 1995.
[29] N. Bambos, S. Chen, and D. Mitra, "Channel probing for distributed access control in wireless communication networks," in *Proc. IEEE GLOBECOM'95*, Singapore, Nov. 1995, pp. 322–326.
[30] N. Bambos, S. C. Chen, and G. J. Pottie, "Radio link admission algorithms for wireless networks with power control and active link quality protection," School of Engineering and Applied Science, Univ. California, Los Angeles, CA, Tech. Rep. UCLA-ENG-94-25, Mar. 1994.

Nicholas Bambos (S'84–M'89) received the Ph.D. degree in electrical engineering and computer science from the University of California, Berkeley, in 1989. He received the engineering Diploma from the Technical University of Athens, Greece, in 1984.

From 1989 to 1995, he was Assistant Professor and later Associate Professor in the Electrical Engineering Department, University of California, Los Angeles. In early 1996, he joined Stanford University, Stanford, CA, as an Associate Professor, where he currently holds a joint appointment in the Electrical Engineering Department and the Management Science and Engineering Department. His current research interests include computer communication network architectures, performance engineering, and stochastic modeling.

Shou C. Chen (S'94–M'95) received the Ph.D. in electrical engineering from the University of California, Los Angeles, in 1994.

He joined Hughes Space and Communications, El Segundo, CA, in 1994. Since 1998 he has been with Trillium Digital Systems, Los Angeles, CA, where he directs a networking group. His research interests include computer communication network architectures and performance engineering.

Gregory J. Pottie (S'85–M'88) was born in Wilmington, DE. He received the B.Sc. degree in engineering physics from Queen's University, Kingston, ON, Canada, in 1984 and the M.Eng. and Ph.D. degrees from McMaster University, Hamilton, ON, in 1985 and 1988, respectively.

From 1989–1991, he was with the Transmission Research Department, Codex/Motorola, Mansfield, MA, where he was involved in high-speed digital subscriber lines and coding and equalization schemes for voice-band modems. He is currently an Associate Professor in the Electrical Engineering Department, University of California, Los Angeles. His research interests include systems design for wireless distributed sensor networks and personal communication transceivers, as well as coding and digital subscriber lines.